LETTER

doi:10.1038/nature24459

Measurement of the multi-TeV neutrino interaction cross-section with IceCube using Earth absorption

The IceCube Collaboration*

Neutrinos interact only very weakly, so they are extremely penetrating. The theoretical neutrino–nucleon interaction cross-section, however, increases with increasing neutrino energy, and neutrinos with energies above 40 teraelectronvolts (TeV) are expected to be absorbed as they pass through the Earth. Experimentally, the cross-section has been determined only at the relatively low energies (below 0.4 TeV) that are available at neutrino beams from accelerators[1,2]. Here we report a measurement of neutrino absorption by the Earth using a sample of 10,784 energetic upward-going neutrino-induced muons. The flux of high-energy neutrinos transiting long paths through the Earth is attenuated compared to a reference sample that follows shorter trajectories. Using a fit to the two-dimensional distribution of muon energy and zenith angle, we determine the neutrino–nucleon interaction cross-section for neutrino energies 6.3–980 TeV, more than an order of magnitude higher than previous measurements. The measured cross-section is about 1.3 times the prediction of the standard model[3], consistent with the expectations for charged- and neutral-current interactions. We do not observe a large increase in the cross-section with neutrino energy, in contrast with the predictions of some theoretical models, including those invoking more compact spatial dimensions[4] or the production of leptoquarks[5]. This cross-section measurement can be used to set limits on the existence of some hypothesized beyond-standard-model particles, including leptoquarks.

The cross-section for neutrino interactions with matter is very small. Neutrinos are usually regarded as particles that will go through anything[6]. However, the neutrino–nucleon interaction cross-section is expected to increase with energy. Until now, the cross-section has only been measured up to a neutrino energy of 370 GeV (Fig. 1; $\log(370) = 2.57$) because it has been limited by the available accelerator neutrino beams[1]. In this range, the cross-section rises linearly with energy.

In the standard model of particle physics, neutrinos interact with quarks through charged-current and neutral-current interactions, mediated by $W^{\pm}$ and Z^0 bosons, respectively. At neutrino energies above 10 TeV, the finite $W^{\pm}$ and Z^0 masses are expected to moderate the increase in cross-section, leading to a slower rise at higher energies. These cross-sections also reflect the densities of partons (quarks and gluons) within the nuclear targets. Accelerator neutrino experiments have mainly probed the densities of partons with Bjorken-x values (the fraction of the total nucleon momentum carried by a quark or gluon) above about 0.1. In this x range, there are more quarks than antiquarks, so the interaction cross-section of the antineutrino is about half that of the neutrino. Higher-energy experiments probe lower Bjorken-x values, where sea quarks predominate, and the difference between the neutrino and antineutrino cross-sections is reduced.

At high energies, new processes beyond the standard model may appear. Some theories invoke new spatial dimensions, which are curled up on a distance scale r. At momentum transfers comparable to $\hbar c/r$, where $\hbar$ is the reduced Planck constant and c is the speed of light in vacuum, the neutrino cross-section rises dramatically[4,7]. In some grand unified or technicolour theories, leptoquarks may couple to both quarks and leptons; for example, a second-generation leptoquark couples to both muon neutrinos and quarks. The interaction cross-section increases considerably at neutrino–quark centre-of-mass energies that correspond to the mass of the leptoquark[5].

Our measurement uses naturally occurring atmospheric and astrophysical neutrinos to extend neutrino interaction cross-section measurements to multi-teraelectronvolt energies by observing neutrino absorption in the Earth. Figure 2 shows the principle of the measurement. Atmospheric neutrinos, produced by cosmic-ray air showers below the Earth's horizon, are the dominant source of neutrinos used for this analysis. Astrophysical neutrinos produced by distant sources are the largest contribution at energies above 300 TeV. High-energy neutrinos that deeply traverse the Earth are absorbed, whereas near-horizontal neutrinos provide an essentially absorption-free reference[9]. The contribution of atmospheric neutrino oscillations is negligible at teraelectronvolt energies and is not included here.

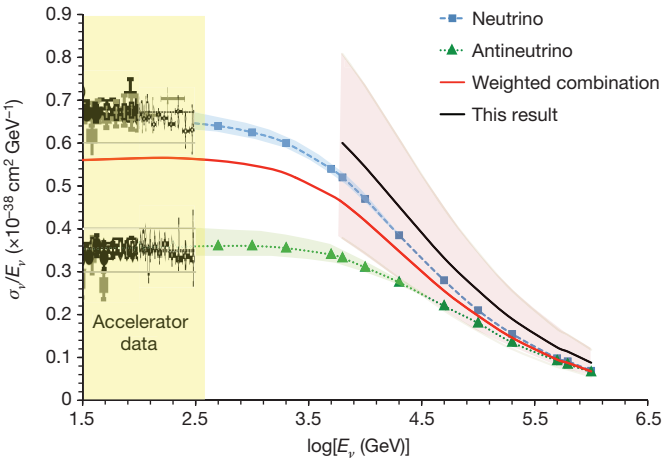

Figure 1 | Neutrino cross-section measurements. Measured neutrino charged-current interaction cross-sections σ_ν, divided by the neutrino energy E_ν, from accelerator experiments are shown, along with error bars showing their combined 1σ statistical and systematic uncertainty, from ref. 1 and from this work. The blue and green lines are the standard model predictions for muon neutrinos ν_μ and antineutrinos $\bar{\nu}_\mu$, respectively, with the uncertainties on the deep-inelastic cross-sections shown by the shaded bands[3]. The red line corresponds to the expected mixture of ν_μ and $\bar{\nu}_\mu$ in the IceCube sample. The black line shows our result, assuming that the charged- and neutral-current cross-sections vary in proportion, and that the ratio between the actual cross-section and the standard model prediction does not depend on energy. The pink band shows the total 1σ (statistical plus systematic) uncertainty. The cross-section increases linearly with energy up to about 3 TeV ($\log(3{,}000) = 3.48$), after which this increase is moderated and the cross-section becomes roughly proportional to $(E_\nu)^{0.3}$ owing to the finite $W^{\pm}$ and Z^0 masses.

*A list of authors and their affiliations appears at the end of the paper.

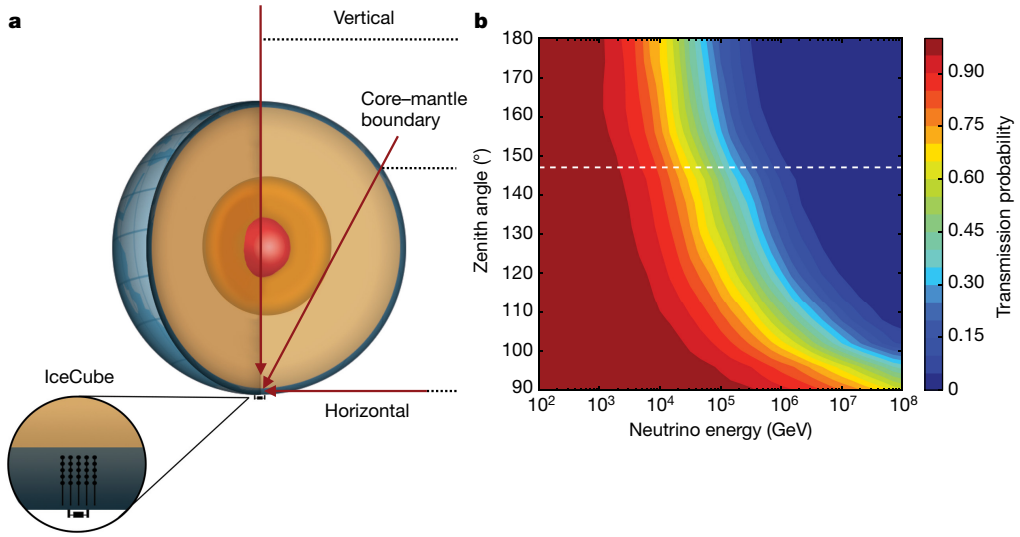

Figure 2 | Neutrino absorption in the Earth. a, Neutrino absorption is observed by measuring how the neutrino energy spectrum changes with the zenith angle. High-energy neutrinos transiting deep through the Earth are absorbed, whereas low-energy neutrinos are not. Neutrinos from just below the horizon provide a nearly absorption-free baseline at all relevant energies. **b**, Standard model prediction for the transmission probability of neutrinos through the Earth as a function of energy and zenith angle. Neutral-current interactions, which occur about 1/3 of the time, are included. When a neutral-current interaction occurs, a neutrino is replaced with one of lower energy. The horizontal white dotted line shows the trajectory (and zenith angle) of a neutrino that just passes through the core–mantle boundary.

The idea of studying neutrino absorption in the Earth dates back to 1974 (ref. 10), although most of the early papers on the subject proposed using absorption to probe the Earth's interior[11]. However, the density uncertainty[12–15] for long paths through the Earth is only 1%–2%; this leads to less than 1% systematic uncertainty in the cross-section measurement, below the total uncertainty of the cross-section. Early work on the subject envisioned using accelerator-produced neutrinos for Earth tomography; the idea of using natural (astrophysical or atmospheric) neutrinos came later[16,17].

Neutrino absorption increases with neutrino energy, so that for 40-TeV neutrinos, the Earth's diameter corresponds to one absorption length. By observing the change in the angular distribution of Earth-transiting neutrinos with increasing neutrino energy, one can measure the increasing absorption and, from that, determine the cross-section.

This analysis uses data collected with the IceCube detector[18], which is installed in the Antarctic ice cap at the South Pole. The data were acquired during 2009 and 2010, when IceCube consisted of 79 vertical strings[19], each supporting 60 optical sensors (Digital Optical Modules, DOMs[20]). The strings are arranged in a triangular grid, with 125 m between strings. The sensors are deployed at 17-m vertical intervals, at depths between 1,450 m and 2,450 m below the surface of the ice cap. Six of the strings are installed at the centre of the array, with smaller string spacing and with their DOMs clustered between 2,100 m and 2,450 m deep; this module is called 'DeepCore'.

The DOMs detect Cherenkov light from the charged particles that are produced when neutrinos interact in the ice surrounding IceCube and the bedrock below. In this measurement, the 79-string detector recorded about 2,000 events per second. About 99.9999% of these were downward-going muons produced directly by cosmic-ray air showers above the horizon. The events were reconstructed using a series of algorithms of increasing accuracy and computational complexity[21,22]. At each stage of processing, a set of conditions was applied to eliminate background events. The final sample of 10,784 upward-going (zenith angle greater than 90°) events had an estimated background of less than 0.1%. Almost all of the background consisted of mis-reconstructed downward-going muons.

The neutrino zenith angles were determined from the reconstructed muon direction. The typical angular resolution was better than 0.6°, including the angular difference between the neutrino and muon directions. This small angular uncertainty does not affect the final result. The neutrino energies were much less well known than the zenith angles because we cannot determine how far from the detector the interaction occurred, so we do not know how much energy the muon lost before entering the detector. Therefore, this analysis used the muon energy as determined from the measured specific energy loss (dE/dx) of the muons. To improve the energy resolution, the muon tracks were divided into 120-m-long segments. The segments with the highest dE/dx values were excluded, and the truncated mean was determined from the remaining segments[23]. The removal of large stochastic losses led to better resolution than that obtained with the untruncated mean. The muon energy values were determined to within roughly a factor of 2.

The cross-section was found by a maximum-likelihood fit, which compared the data, binned by zenith angle and muon energy, with a model that included contributions from atmospheric and astrophysical neutrinos. The cross-section entered the fit through the energy- and zenith-angle-dependent probability for the neutrinos to be absorbed as they pass through the Earth. This absorption probability depends on the nucleon density, integrated along the path of the neutrino through the Earth. We used the Preliminary Reference Earth Model to determine the density of the Earth[12]. Thanks to seismic wave studies and tight constraints on the total mass of the Earth, the uncertainties in the integrated density were lower than a few per cent.

To account for neutral-current interactions, in which neutrinos lose a fraction of their energy, we modelled neutrino transmission through the Earth at each zenith angle in two dimensions: the incident neutrino energy and the neutrino energy near IceCube. The fit determined $R = \sigma_{meas}/\sigma_{SM}$, where σ_{meas} is the measured cross-section and σ_{SM} is the standard model cross-section from ref. 3. That calculation used quark and gluon densities derived from the Hydrogen Epoch of Reionization Array (HERA) data to find the interaction cross-sections of neutrinos and antineutrinos with protons and neutrons, treating the Earth as an isoscalar target. The estimated uncertainty in the calculation was less than 5% for the energy range covered by this analysis. Because the calculation did not include nuclear shadowing, it might overestimate the cross-section for heavier elements, such as the iron in the core of the Earth. Experiments with 2–22-GeV neutrinos interacting with iron targets[24] and 20–300-GeV neutrinos interacting with neon[25] did not observe nuclear shadowing, but it may be present for higher-energy neutrinos[26].

The fitted charged-current and neutral-current cross-sections were assumed to be the same multiples of their standard model counterparts,

Table 1 | Fitting parameters for the cross-section fit

Result	Baseline	Nuisance parameter input and uncertainty	Nuisance parameter fit result and uncertainty
$\Phi_{conv} \times \sigma$	Ref. 27 $\times R$	1.0 ± 0.25	0.92 ± 0.03
Φ_{conv} spectral index	Ref. 27 with knee	0.00 ± 0.05	0.007 ± 0.001
K/π ratio	Ref. 27 baseline	1.0 ± 0.1	1.05 ± 0.09
$\nu/\bar{\nu}$ ratio	Ref. 27 baseline	1.0 ± 0.1	1.01 ± 0.005
$\Phi_{prompt} \times \sigma$	Ref. 28 $\times R$	$0.0^{+1.0}_{-0.0}$	$0.5^{+0.40}_{-0.34}$
$\Phi_{astro} \times \sigma$	Ref. 8 $\times R$	2.23 ± 0.4	$2.62^{+0.05}_{-0.07}$
γ		-2.50 ± 0.09	-2.42 ± 0.02
DOM efficiency	IceCube baseline	1.0 ± 0.1	1.05 ± 0.01

The fitting parameters with their baseline are shown in the second column, along with the initial assumption and uncertainty input to the fit (third column) and the values returned by the fit (last column). The neutrino fluxes are for ν_μ and $\bar{\nu}_\mu$ only. For the astrophysical component, the baseline flux is $\Phi_{astro} \times (E_\nu/100\ \text{TeV})^\gamma\ 10^{-18}\ \text{s}^{-1}\ \text{cm}^{-2}\ \text{sr}^{-1}$. The three flux terms are multiplied by R ($R = \sigma_{meas}/\sigma_{SM}$) to remove the obvious linear correlation between the number of observed events and the cross-section, which exists even in the absence of absorption. γ is the astrophysical index, Φ_{conv} is the conventional atmospheric flux and Φ_{prompt} is the prompt atmospheric flux.

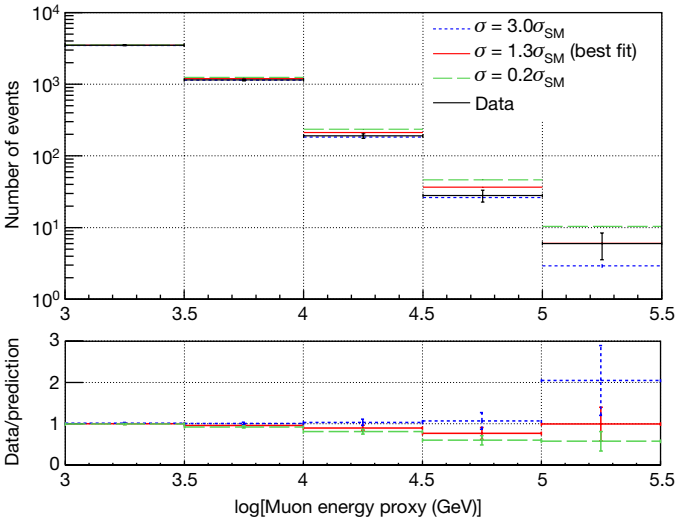

Figure 3 | Cross-section data compared with Monte Carlo model predictions. Energy spectrum of the data (black points) and the best-fit results (red curve) with the cross-sections fixed to 0.2 (green) and 3.0 (blue) times that predicted by the standard model for events with zenith angles between 110° and 180°, where absorption is substantial, are shown in the top panel. The bottom panel shows the ratios of the data to the three Monte Carlo predictions. The error bars show the 1σ (statistical only) errors.

and we ignored nuclear shadowing. The fitting procedure was repeated for different cross-section values (varying in steps of $\Delta R = 0.2$), leading to a parabolic curve of likelihood versus cross-section.

The flux model included conventional atmospheric neutrinos from $\pi^\pm$ and $K^\pm$ decay, prompt atmospheric neutrinos from the decay of charm/bottom hadrons and astrophysical neutrinos. Because the precise neutrino fluxes and spectra were imperfectly known, they were included as nuisance parameters in the fit, with the initial values and Gaussian uncertainties shown in Table 1. Five parameters accounted for the atmospheric, prompt and astrophysical neutrino fluxes (Φ) and two spectral indices, for the atmospheric and astrophysical fluxes (the prompt index is kept fixed). The other parameters were the kaon-to-pion (K/π) and muon neutrino-to-antineutrino ($\nu_\mu/\bar{\nu}_\mu$) ratios in cosmic-ray air showers, plus one parameter to account for the overall optical efficiency of the IceCube DOMs.

We used previous conventional and prompt atmospheric neutrino spectra from cosmic-ray air-shower simulations that were obtained from lower-energy neutrino data[27] and a colour dipole model calculation[28], respectively. We modified these spectra to account for the steepening of the cosmic-ray spectrum at the 'knee'[29] (a steepening of the cosmic-ray spectrum at a cosmic-ray energy of around 3 PeV). Recent perturbative quantum chromodynamics calculations[30–32] have found a lower prompt flux than in ref. 26. However, the prompt component is small and has little effect on this analysis, and the fitting results are compatible with both calculations and with existing upper limits[29] on the prompt flux. Finally, the astrophysical spectrum was obtained on the basis of a recent combined fit[8]. There is some disagreement between the spectral index derived from the combined fit and that obtained from a newer analysis[29], which was focused on through-going muon tracks from muon neutrinos (ν_μ); this discrepancy was treated as a systematic uncertainty that was due to the uncertain spectral index.

Because past measurements of the neutrino flux were based on the assumption that the standard model cross-section is correct, this fit uses the product of each flux with that cross-section to apply constraints directly from the previous data. As the cross-section rises, the fluxes must drop to preserve the total number of events observed in previous experiments. The fit is thus sensitive to neutrino absorption in the Earth, and not to the total number of observed events.

The fit finds a cross-section $1.30^{+0.30}_{-0.26}$ times that of the standard model. The uncertainty is a mixture of the statistical uncertainty and the systematic errors from the uncertainties in the nuisance parameters. We isolate the statistical error by refitting with the nuisance parameters fixed to their preferred values, and find a statistical error of $^{+0.21}_{-0.19}$. The remainder of the fitting error, $^{+0.21}_{-0.18}$ after quadrature subtraction, is attributed to systematic uncertainty sources in the fit.

Figure 3 compares the measured muon energy proxy spectrum for zenith angles between 110° and 180° (where absorption is substantial) with three fits: the best-fit result (using the cross-section given above) and two comparison fits with cross-sections 0.2 and 3.0 times the standard model prediction. The spectrum steepens noticeably as the cross-section increases. We use the term 'energy proxy' because of the limited energy resolution.

The other major detector-related uncertainty is due to the optical properties of ice. This was studied with separate dedicated simulations, in which the scattering and absorption lengths were varied by ±10%. This led to a systematic uncertainty of $^{+0.30}_{-0.38}$ in the standard model cross-section. Four other systematic uncertainties were considered: uncertainty in the density distribution of the Earth[13–15] (±0.01), variations in atmospheric pressure at the neutrino production sites[9] $\left(^{+0.00}_{-0.04}\right)$, uncertainties in the prompt and astrophysical neutrino spectral indices (±0.10) and uncertainties in the angular acceptance of the IceCube DOMs $\left(^{+0.04}_{-0.00}\right)$. These systematic errors were then added in quadrature to the systematic uncertainties from the fit, giving a total systematic uncertainty of $^{+0.39}_{-0.43}$ times the prediction of the standard model.

The neutrino energy range in which this analysis is relevant was found by repeating the fit procedure with the absorption probability set to zero for neutrino energies below a certain threshold. As the threshold was gradually increased, the data and simulation diverged, and the quality of the fit was degraded. The threshold that corresponded to a likelihood increase of 1.0σ ($-2\Delta\text{LLH} = 1$, where ΔLLH is the change in the natural logarithm of the likelihood) was the minimum energy to which this analysis was sensitive. We repeated the process by turning off neutrino absorption above a gradually decreasing high-energy threshold to find the upper end of the energy range and obtained the energy range 6.3–980 TeV. This wide range reflects the combination of a neutrino flux that decreases rapidly with energy (partially compensated by an increasing cross-section and detection probability) with the relatively rapid increase in absorption with increasing energy.

Figure 1 compares this measurement with previous measurements of neutrino cross-sections made at accelerator facilities. Ours is the first cross-section measurement at multi-teraelectronvolt energies, at which the effects of the finite $W^\pm$ and Z^0 masses slow the increase of the cross-section with increasing energy. We measured the cross-section to be $1.30^{+0.21}_{-0.19}$ (statistical uncertainty) $^{+0.39}_{-0.43}$ (systematic uncertainty)

times the prediction of the standard model for charged- and neutral-current interactions in the energy range from 6.3 TeV to 980 TeV ($\log[E_\nu\ (\mathrm{GeV})] = 3.8–6.0$). We did not see a dramatic increase in cross-section, as predicted by models of beyond-standard-model physics, such as those involving extra dimensions[4] or leptoquarks[5].

Future optical Cherenkov experiments with IceCube or larger detectors, such as IceCube-Gen2[33] or Phase 2.0 of KM3NeT[34], should be able to extend this measurement to higher energies and study the energy dependence of the interaction cross-section of neutrinos. Future experiments that detect the radio emission from neutrino showers over volumes exceeding 100 km^3 using the ARA and ARIANNA technologies[35,36] could observe the interactions of GZK neutrinos and extend the cross-section measurements up to energies of 10^{19} eV (ref. 37). Experiments at these energies will have sensitivity to phenomena (very heavy leptoquarks, or additional dimensions with small spatial extent) beyond the standard model that occur at higher energies than those that can be probed at CERN's Large Hadron Collider.

Online Content Methods, along with any additional Extended Data display items and Source Data, are available in the online version of the paper; references unique to these sections appear only in the online paper.

Received 20 July; accepted 20 September 2017.
Published online 22 November 2017.

1. Olive, K. A. *et al.* Review of particle physics. *Chin. Phys. C* **38,** 090001 (2014).
2. Formaggio, J. A. & Zeller, G. P. From eV to EeV: neutrino cross sections across energy scales. *Rev. Mod. Phys.* **84,** 1307–1341 (2012).
3. Cooper-Sarkar, A., Mertsch, P. & Sarkar, S. The high energy neutrino cross-section in the Standard Model and its uncertainty. *J. High Energy Phys.* **2011,** 42 (2011).
4. Alvarez-Muñiz, J., Feng, J. L., Halzen, F., Han, T. & Hooper, D. Detecting microscopic black holes with neutrino telescopes. *Phys. Rev. D* **65,** 124015 (2002).
5. Romero, I. & Sampayo, O. A. Leptoquarks signals in KM^3 neutrino telescopes. *J. High Energy Phys.* **2009,** 111 (2009).
6. Sutton, C. *Spaceship Neutrino* (Cambridge Univ. Press, 1992).
7. Connolly, A., Thorne, R. S. & Waters, D. Calculation of high energy neutrino–nucleon cross sections and uncertainties using the Martin–Stirling–Thorne–Watt parton distribution functions and implications for future experiments. *Phys. Rev. D* **83,** 113009 (2011).
8. IceCube Collaboration. A combined maximum-likelihood analysis of the high-energy astrophysical neutrino flux measured with IceCube. *Astrophys. J.* **809,** 98 (2015).
9. Miarecki, S. C. *Earth versus Neutrinos: Measuring the Total Muon-Neutrino-to-Nucleon Cross Section at Ultra-high Energies through Differential Earth Absorption of Muon Neutrinos from Cosmic Rays using the IceCube Detector.* PhD thesis, Univ. California, Berkeley https://docushare.icecube.wisc.edu/dsweb/Get/Document-78967/dissertation_Miarecki_2016.pdf (2016).
10. Volkova, L. V. & Zatsepin, G. T. Passage of neutrinos through the Earth. *Bull. Acad. Sci. USSR Phys. Ser.* **38,** 151–154 (1974); translated from *Izv. Akad. Nauk SSSR, Ser. fiz.* **38,** 1060–1063 (1974).
11. Wilson, T. L. Neutrino tomography: tevatron mapping versus the neutrino sky. *Nature* **309,** 38–42 (1984).
12. Dziewonski, A. M. & Anderson, D. L. Preliminary reference Earth model. *Phys. Earth Planet. Inter.* **25,** 297–356 (1981).
13. Kennett, B. L. N. On the density distribution within the Earth. *Geophys. J. Int.* **132,** 374–382 (1998).
14. Masters, G. & Gubbins, D. On the resolution of density within the Earth. *Phys. Earth Planet. Inter.* **140,** 159–167 (2003).
15. de Wit, R. W. L., Käufl, P. J., Valentine, A. P. & Trampert, J. Bayesian inversion of free oscillations for Earth's radial (an)elastic structure. *Phys. Earth Planet. Inter.* **237,** 1–17 (2014).
16. Dumand Collaboration. Mapping the Earth's interior with astrophysical neutrinos. In *24th International Cosmic Ray Conference* Vol. 1 (eds Iucci, N. & Lamanna, E.) 804–807 http://adsabs.harvard.edu/full/1995ICRC....1..804D (IUPAP, 1995).
17. Gonzalez-Garcia, M. C., Halzen, F., Maltoni, M. & Tanaka, H. K. M. Radiography of Earth's core and mantle with atmospheric neutrinos. *Phys. Rev. Lett.* **100,** 061802 (2008).
18. IceCube Collaboration. The IceCube neutrino observatory: instrumentation and online systems. *J. Instrum.* **12,** P03012 (2017).
19. Halzen, F. & Klein, S. R. IceCube: an instrument for neutrino astronomy. *Rev. Sci. Instrum.* **81,** 081101 (2010).
20. IceCube Collaboration. The IceCube data acquisition system: signal capture, digitization, and timestamping. *Nucl. Instrum. Meth. A* **601,** 294–316 (2009).
21. IceCube Collaboration. Evidence for astrophysical muon neutrinos from the northern sky with IceCube. *Phys. Rev. Lett.* **115,** 081102 (2015).
22. Weaver, C. *Evidence for Astrophysical Muon Neutrinos from the Northern Sky.* PhD thesis, Univ. Wisconsin https://docushare.icecube.wisc.edu/dsweb/Get/Document-73829/weaver_thesis_2015.pdf (2015).
23. IceCube Collaboration. An improved method for measuring muon energy using the truncated mean of dE/dx. *Nucl. Instrum. Meth. A* **703,** 190–198 (2013).
24. MINERvA Collaboration. Measurement of partonic nuclear effects in deep-inelastic neutrino scattering using MINERvA. *Phys. Rev. D* **93,** 071101 (2016).
25. WA25 and WA59 Collaborations. An investigation of the EMC effect using anti-neutrinos interactions in deuterium and neon. *Phys. Lett.* **141,** 133–139 (1984).
26. Eskola, K. J., Paakkinen, P., Paukkunen, H. & Salgado, C. A. EPPS16: nuclear parton distributions with LHC data. *Eur. Phys. J. C* **77,** 163 (2017).
27. Honda, M., Kajita, T., Kasahara, K., Midorikawa, S. & Sanuki, T. Calculation of atmospheric neutrino flux using the interaction model calibrated with atmospheric muon data. *Phys. Rev. D* **75,** 043006 (2007).
28. Enberg, R., Reno, M. H. & Sarcevic, I. High energy neutrinos from charm in astrophysical sources. *Phys. Rev. D* **79,** 053006 (2009).
29. IceCube Collaboration. Observation and characterization of a cosmic muon neutrino flux from the northern hemisphere using six years of IceCube data. *Astrophys. J.* **833,** 3 (2016).
30. Bhattacharya, A., Enberg, R., Reno, M. H., Sarcevic, I. & Stasto, A. Perturbative charm production and the prompt atmospheric neutrino flux in light of RHIC and LHC. *J. High Energy Phys.* **1506,** 110 (2015).
31. Garzelli, M. V., Moch, S. & Sigl, G. Lepton fluxes from atmospheric charm revisited. *J. High Energy Phys.* **1510,** 115 (2015).
32. Gauld, R., Rojo, J., Rottoli, L., Sarkar, S. & Talbert, J. The prompt atmospheric neutrino flux in the light of LHCb. *J. High Energy Phys.* **1602,** 130 (2016).
33. IceCube-Gen2 Collaboration. IceCube-Gen2: a vision for the future of neutrino astronomy in Antarctica. Preprint at https://arxiv.org/abs/1412.5106 (2014).
34. KM3Net Collaboration. Letter of intent for KM3NeT 2.0. *J. Phys. G* **43,** 084001 (2016).
35. ARIANNA Collaboration. A first search for cosmogenic neutrinos with the ARIANNA hexagonal radio array. *Astropart. Phys.* **70,** 12 (2015).
36. ARA Collaboration. Performance of two Askaryan Radio Array stations and first results in the search for ultrahigh energy neutrinos. *Phys. Rev. D* **93,** 082003 (2016).
37. Klein, S. R. & Connolly, A. Neutrino absorption in the Earth, neutrino cross-sections, and new physics. Preprint at https://arxiv.org/abs/1304.4891 (2013).

Acknowledgements We acknowledge support from the following agencies: United States Air Force Academy, US National Science Foundation, Office of Polar Programs; US National Science Foundation, Physics Division; University of Wisconsin Alumni Research Foundation; the Grid Laboratory of Wisconsin (GLOW) grid infrastructure at the University of Wisconsin, Madison; the Open Science Grid (OSG) grid infrastructure; US Department of Energy; National Energy Research Scientific Computing Center; the Louisiana Optical Network Initiative (LONI) grid computing resources; Natural Sciences and Engineering Research Council of Canada; WestGrid and Compute/Calcul Canada; Swedish Research Council; Swedish Polar Research Secretariat; Swedish National Infrastructure for Computing (SNIC); Knut and Alice Wallenberg Foundation; German Ministry for Education and Research (BMBF); Deutsche Forschungsgemeinschaft (DFG); Helmholtz Alliance for Astroparticle Physics (HAP); Initiative and Networking Fund of the Helmholtz Association, Germany; Fund for Scientific Research (FNRS-FWO), FWO Odysseus programme, Flanders Institute to encourage scientific and technological research in industry (IWT), Belgian Federal Science Policy Office (BELSPO); Marsden Fund; Australian Research Council; Japan Society for Promotion of Science (JSPS); Swiss National Science Foundation (SNSF); National Research Foundation of Korea (NRF); Villum Fonden, Danish National Research Foundation (DNRF).

Author Contributions The IceCube neutrino observatory was designed and constructed by the IceCube Collaboration and the IceCube Project, which continues to operate it. Data processing and calibration, Monte Carlo simulations of the detector and of theoretical models, and data analyses were performed by a large number of IceCube Collaboration members, who also discussed and approved the scientific results. The analysis presented here was performed by S.Mi. with input from G.B. The paper was written by S.Mi., G.B. and S.R.K. and reviewed by the collaboration. All authors approved the final version of the manuscript.

Author Information Reprints and permissions information is available at www.nature.com/reprints. The authors declare no competing financial interests. Readers are welcome to comment on the online version of the paper. Publisher's note: Springer Nature remains neutral with regard to jurisdictional claims in published maps and institutional affiliations. Correspondence and requests for materials should be addressed to S.R.K. (srklein@lbl.gov).

Reviewer Information *Nature* thanks A. De Gouvea and the other anonymous reviewer(s) for their contribution to the peer review of this work.

The IceCube Collaboration

M. G. Aartsen[1], G. C. Hill[1], A. Kyriacou[1], S. Robertson[1], A. Wallace[1], B. J. Whelan[1], M. Ackermann[2], E. Bernardini[2], S. Blot[2], F. Bradascio[2], H.-P. Bretz[2], J. Brostean-Kaiser[2], A. Franckowiak[2], E. Jacobi[2], T. Karg[2], T. Kintscher[2], S. Kunwar[2], R. Nahnhauer[2], K. Satalecka[2], C. Spiering[2], J. Stachurska[2], A. Stasik[2], N. L. Strotjohann[2], A. Terliuk[2], M. Usner[2], J. van Santen[2], J. Adams[3], H. Bagherpour[3], J. A. Aguilar[4], I. Ansseau[4], D. Heereman[4], K. Meagher[4], T. Meures[4], A. O'Murchadha[4], E. Pinat[4], C. Raab[4], M. Ahlers[5], D. J. Koskinen[5], M. J. Larson[5], M. Medici[5], M. Rameez[5], M. Ahrens[6,7], C. Bohm[6,7], J. P. Dumm[6,7], C. Finley[6,7], S. Flis[6,7], K. Hultqvist[6,7], C. Walck[6,7], M. Zoll[6,7], I. Al Samarai[8], S. Bron[8], T. Carver[8], A. Christov[8], T. Montaruli[8], D. Altmann[9], G. Anton[9], T. Glüsenkamp[9], U. Katz[9], T. Kittler[9], M. Tselengidou[9], K. Andeen[10], M. Plum[10], T. Anderson[11], J. J. DeLaunay[11], M. Dunkman[11], P. Eller[11], F. Huang[11], A. Keivani[11], J. L. Lanfranchi[11], D. V. Pankova[11], G. Tešić[11], C. F. Turley[11], M. J. Weiss[11], C. Argüelles[12], S. Axani[12], G. H. Collin[12], J. M. Conrad[12], M. Moulai[12], J. Auffenberg[13], M. Brenzke[13], T. Glauch[13], C. Haack[13], P. Kalaczynski[13], J. P. Koschinsky[13], M. Leuermann[13], L. Rädel[13], R. Reimann[13], M. Rongen[13], T. Sälzer[13], S. Schoenen[13], L. Schumacher[13], J. Stettner[13], M. Vehring[13], E. Vogel[13], M. Wallraff[13], A. Waza[13], C. H. Wiebusch[13], X. Bai[14], J. P. Barron[15], W. Giang[15], D. Grant[15], C. Kopper[15], R. W. Moore[15], S. C. Nowicki[15], S. E. Sanchez Herrera[15], S. Sarkar[15], F. D. Wandler[15], C. Weaver[15], T. R. Wood[15], E. Woolsey[15], J. P. Yanez[15], S. W. Barwick[16], G. Yodh[16], V. Baum[17], S. Böser[17], V. di Lorenzo[17], B. Eberhardt[17], T. Ehrhardt[17], L. Köpke[17], G. Krückl[17], G. Momenté[17], P. Peiffer[17], J. Sandroos[17], A. Steuer[17], K. Wiebe[17], R. Bay[18], K. Filimonov[18], P. B. Price[18], K. Woschnagg[18], J. J. Beatty[19,20], J. Becker Tjus[21], F. Bos[21], B. Eichmann[21], M. Kroll[21], S. Schöneberg[21], F. Tenholt[21], K.-H. Becker[22], D. Bindig[22], K. Helbing[22], S. Hickford[22], R. Hoffmann[22], F. Lauber[22], U. Naumann[22], A. Obertacke Pollmann[22], D. Soldin[22], S. BenZvi[23], R. Cross[23], D. Berley[24], E. Blaufuss[24], E. Cheung[24], J. Felde[24], E. Friedman[24], R. Hellauer[24], K. D. Hoffman[24], R. Maunu[24], A. Olivas[24], T. Schmidt[24], M. Song[24], G. W. Sullivan[24], D. Z. Besson[25], G. Binder[18,26], S. R. Klein[18,26], S. Miarecki[18,26], T. Palczewski[18,26], J. Tatar[18,26], M. Börner[27], T. Fuchs[27], M. Hünnefeld[27], M. Meier[27], T. Menne[27], D. Pieloth[27], W. Rhode[27], T. Ruhe[27], A. Sandrock[27], P. Schlunder[27], J. Soedingrekso[27], J. Werthebach[27], D. Bose[28], H. Dujmovic[28], S. In[28], M. Jeong[28], W. Kang[28], J. Kim[28], C. Rott[28], O. Botner[29], A. Burgman[29], A. Hallgren[29], C. Pérez de los Heros[29], E. Unger[29], J. Bourbeau[30], J. Braun[30], J. Casey[30], D. Chirkin[30], M. Day[30], P. Desiati[30], J. C. Díaz-Vélez[30], S. Fahey[30], K. Ghorbani[30], Z. Griffith[30], F. Halzen[30], K. Hanson[30], B. Hokanson-Fasig[30], K. Hoshina[30,31], K. Jero[30], A. Karle[30], M. Kauer[30], J. L. Kelley[30], A. Kheirandish[30], Q. R. Liu[30], W. Luszczak[30], S. Mancina[30], F. McNally[30], G. Merino[30], A. Schneider[30], M. N. Tobin[30], D. Tosi[30], B. Ty[30], J. Vandenbroucke[30], N. Wandkowsky[30], C. Wendt[30], S. Westerhoff[30], L. Wille[30], M. Wolf[30], J. Wood[30], D. L. Xu[30], T. Yuan[30], L. Brayeur[32], M. Casier[32], C. De Clercq[32], K. D. de Vries[32], G. de Wasseige[32], J. Kunnen[32], J. Lünemann[32], G. Maggi[32], S. Toscano[32], N. van Eijndhoven[32], K. Clark[33], L. Classen[34], A. Kappes[34], S. Coenders[35], M. Huber[35], K. Krings[35], I. C. Rea[35], E. Resconi[35], A. Turcati[35], D. F. Cowen[36,37], J. P. A. M. de André[38], T. DeYoung[38], J. Hignight[38], D. Lennarz[38], K. B. M. Mahn[38], J. Micallef[38], G. Neer[38], D. Rysewyk[38], H. Dembinski[39], P. A. Evenson[39], T. K. Gaisser[39], J. G. Gonzalez[39], R. Koirala[39], H. Pandya[39], D. Seckel[39], T. Stanev[39], S. Tilav[39], S. De Ridder[40], M. Labare[41], D. Ryckbosch[41], W. Van Driessche[41], S. Vanheule[41], M. Vraeghe[41], M. de With[41], D. Hebecker[41], H. Kolanoski[41], A. R. Fazely[42], S. Ter-Antonyan[42], X. W. Xu[42], J. Gallagher[43], L. Gerhardt[26], A. Goldschmidt[26], D. R. Nygren[26], G. T. Przybylski[26], T. Stezelberger[26], R. G. Stokstad[26], A. Ishihara[44], M. Kim[44], T. Kuwabara[44], L. Lu[44], K. Mase[44], M. Relich[44], A. Stößl[44], S. Yoshida[44], G. S. Japaridze[45], B. J. P. Jones[46], J. Kiryluk[47], M. Lesiak-Bzdak[47], H. Niederhausen[47], Y. Xu[47], G. Kohnen[48], S. Kopper[49], P. Nakarmi[49], J. A. Pepper[49], P. A. Toale[49], D. R. Williams[49], M. Kowalski[2,41], N. Kurahashi[50], B. Relethford[50], M. Richman[50], L. Wills[50], J. Madsen[51], S. Seunarine[51], G. M. Spiczak[51], R. Maruyama[52], K. Rawlins[53], S. Sarkar[5,54], M. Sutherland[19], I. Taboada[55] & C. F. Tung[55]

[1]Department of Physics, University of Adelaide, Adelaide 5005, Australia. [2]DESY, D-17738 Zeuthen, Germany. [3]Department of Physics and Astronomy, University of Canterbury, Private Bag 4800, Christchurch, New Zealand. [4]Université Libre de Bruxelles, Science Faculty CP230, B-1050 Brussels, Belgium. [5]Niels Bohr Institute, University of Copenhagen, DK-2100 Copenhagen, Denmark. [6]Oskar Klein Centre, Stockholm University, SE-10691 Stockholm, Sweden. [7]Department of Physics, Stockholm University, SE-10691 Stockholm, Sweden. [8]Département de physique nucléaire et corpusculaire, Université de Genève, CH-1211 Genève, Switzerland. [9]Erlangen Centre for Astroparticle Physics, Friedrich-Alexander-Universität Erlangen-Nürnberg, D-91058 Erlangen, Germany. [10]Department of Physics, Marquette University, Milwaukee, Wisconsin 53201, USA. [11]Department of Physics, Pennsylvania State University, University Park, Pennsylvania 16802, USA. [12]Department of Physics, Massachusetts Institute of Technology, Cambridge, Massachusetts 02139, USA. [13]III. Physikalisches Institut, RWTH Aachen University, D-52056 Aachen, Germany. [14]Physics Department, South Dakota School of Mines and Technology, Rapid City, South Dakota 57701, USA. [15]Department of Physics, University of Alberta, Edmonton, Alberta T6G 2E1, Canada. [16]Department of Physics and Astronomy, University of California, Irvine, California 92697, USA. [17]Institute of Physics, University of Mainz, Staudinger Weg 7, D-55099 Mainz, Germany. [18]Department of Physics, University of California, Berkeley, California 94720, USA. [19]Department of Physics and Center for Cosmology and Astro-Particle Physics, Ohio State University, Columbus, Ohio 43210, USA. [20]Department of Astronomy, Ohio State University, Columbus, Ohio 43210, USA. [21]Fakultät für Physik & Astronomie, Ruhr-Universität Bochum, D-44780 Bochum, Germany. [22]Department of Physics, University of Wuppertal, D-42119 Wuppertal, Germany. [23]Department of Physics and Astronomy, University of Rochester, Rochester, New York 14627, USA. [24]Department of Physics, University of Maryland, College Park, Maryland 20742, USA. [25]Department of Physics and Astronomy, University of Kansas, Lawrence, Kansas 66045, USA. [26]Lawrence Berkeley National Laboratory, Berkeley, California 94720, USA. [27]Department of Physics, TU Dortmund University, D-44221 Dortmund, Germany. [28]Department of Physics, Sungkyunkwan University, Suwon 440-746, Korea. [29]Department of Physics and Astronomy, Uppsala University, Box 516, S-75120 Uppsala, Sweden. [30]Department of Physics and Wisconsin IceCube Particle Astrophysics Center, University of Wisconsin, Madison, Wisconsin 53706, USA. [31]Earthquake Research Institute, University of Tokyo, Bunkyo, Tokyo 113-0032, Japan. [32]Vrije Universiteit Brussel (VUB), Dienst ELEM, B-1050 Brussels, Belgium. [33]SNOLAB, 1039 Regional Road 24, Creighton Mine 9, Lively, Ontario P3Y 1N2, Canada. [34]Institut für Kernphysik, Westfälische Wilhelms-Universität Münster, D-48149 Münster, Germany. [35]Physik-department, Technische Universität München, D-85748 Garching, Germany. [36]Department of Physics, Pennsylvania State University, University Park, Pennsylvania 16802, USA. [37]Department of Astronomy and Astrophysics, Pennsylvania State University, University Park, Pennsylvania 16802, USA. [38]Department of Physics and Astronomy, Michigan State University, East Lansing, Michigan 48824, USA. [39]Bartol Research Institute and Department of Physics and Astronomy, University of Delaware, Newark, Delaware 19716, USA. [40]Department of Physics and Astronomy, University of Gent, B-9000 Gent, Belgium. [41]Institut für Physik, Humboldt-Universität zu Berlin, D-12489 Berlin, Germany. [42]Department of Physics, Southern University, Baton Rouge, Louisiana 70813, USA. [43]Department of Astronomy, University of Wisconsin, Madison, Wisconsin 53706, USA. [44]Department of Physics and Institute for Global Prominent Research, Chiba University, Chiba 263-8522, Japan. [45]Center for Theoretical Studies in Physical Systems, Clark-Atlanta University, Atlanta, Georgia 30314, USA. [46]Department of Physics, University of Texas at Arlington, 502 Yates Street, Science Hall Room 108, Box 19059, Arlington, Texas 76019, USA. [47]Department of Physics and Astronomy, Stony Brook University, Stony Brook, New York 11794-3800, USA. [48]Université de Mons, 7000 Mons, Belgium. [49]Department of Physics and Astronomy, University of Alabama, Tuscaloosa, Alabama 35487, USA. [50]Department of Physics, Drexel University, 3141 Chestnut Street, Philadelphia, Pennsylvania 19104, USA. [51]Department of Physics, University of Wisconsin, River Falls, Wisconsin 54022, USA. [52]Department of Physics, Yale University, New Haven, Connecticut 06520, USA. [53]Department of Physics and Astronomy, University of Alaska Anchorage, 3211 Providence Drive, Anchorage, Alaska 99508, USA. [54]Department of Physics, University of Oxford, 1 Keble Road, Oxford OX1 3NP, UK. [55]School of Physics and Center for Relativistic Astrophysics, Georgia Institute of Technology, Atlanta, Georgia 30332, USA.

METHODS

The dataset used in this analysis was collected between 31 May 2010 and 13 May 2011, when the IceCube detector consisted of 79 strings. The data were processed with the standard IceCube calibration and reconstruction algorithms[22], including energy determination using the truncated mean method[9]. A series of event selection criteria were applied to accept well-reconstructed upward-going track events with reconstructed muon-energy proxy[22] above 1 TeV.

The events were then two-dimensionally binned in terms of zenith angle and muon-energy proxy and fitted by the combination of simulated events described in the main text. The simulated events were generated with standard IceCube programs that simulated the flux of neutrinos propagated through the Earth and forced to interact in or near IceCube. The resulting particle showers were simulated and reconstructed using standard IceCube simulation programs. Simulations were run for several assumed neutrino cross-sections, as described in the main text, and the results were interpolated between these cross-sections. Uncertainties in the different neutrino flux parameters listed in Table 1 were accounted for by using a weighting scheme for the simulated events. By adjusting the event weightings, different spectra could be simulated without rerunning the simulations.

Code availability. Proprietary codes used are embedded within the IceCube simulation framework and the IceTray framework. It is not practical to separate these and the codes are not therefore publicly available.

Data availability. The data used in this analysis are available online at http://icecube.wisc.edu/science/data/HE_NuMu_diffuse. The data were collected before 13 May 2011 (before run number 118175)[22]. That data release uses an energy proxy that is similar to, but not identical to, that used for the current analysis.